Talanta 146 (2016) 285–290

Contents lists available at ScienceDirect

Talanta

journal homepage: www.elsevier.com/locate/talanta

A novel biosensor based on Au@Ag core–shell nanoparticles for SERS detection of arsenic (III)

Lulu Song [a,1], Kang Mao [a,b,1], Xiaodong Zhou [a,*], Jiming Hu [a]

[a] Key Laboratory of Analytical Chemistry for Biology and Medicine (Ministry of Education), College of Chemistry and Molecular Sciences, Wuhan University, Wuhan 430072, China

[b] Laboratory for Earth Surface Processes, College of Urban and Environmental Sciences, Peking University, Beijing 100871, China

ARTICLE INFO

Article history:
Received 23 June 2015
Received in revised form
16 August 2015
Accepted 24 August 2015
Available online 28 August 2015

Keywords:
As (III)
Au@Ag
As (III) -aptamer
SERS

ABSTRACT

In this work, we propose for the first time a simple and novel approach based on SERS and As (III) -aptamer for detection of As (III) with excellent selectivity and sensitivity. To maintain the wonderful SERS substrate, Au@Ag shell–core nanoparticle has been successfully synthesized by seeds growth method. As-prepared Au@Ag not only has well-dispersed but also obtains high SERS efficiency. The novel As (III) biosensor has an excellent linear correlation with the concentration of As (III) ranging from 0.5 to 10 ppb. The detection limit of this assay for As (III) is 0.1 ppb (3 times standard deviation rules) which is lower than the maximum limitation guided by the United States Environmental Protection Agency (EPA) and the World Health Organization (WHO). Importantly, the results were demonstrated that no other ions interfered with the detection of As (III) in water. Further, this As (III) biosensor was demonstrated in monitoring As (III) in lake water samples with satisfactory results.

1. Introduction

As one of the most toxic heavy metals, arsenic is widely distributed in the environment, not only causing severe environmental pollution, but also producing serious adverse effects on human health [1–5]. Nowadays, arsenic pollution in natural waters has become a global environmental issue and has been frequently reported in many countries and regions [1,6–13]. Arsenate [As (V)] and arsenite [As (III)] are the most common forms of arsenic species existing in aqueous environments [3]. Humans are likely to ingest arsenic if they are directly or indirectly exposed to arsenic, drinking arsenic-laden water and eating crops grown from arsenic-accumulated soils [14]. Due to the acute or chronic toxic effects of arsenic, long-term ingestion or exposure to arsenic can lead to various types of cancer [15], skin lesions [16], arsenicosis [17] and cardio-vascular diseases [18]. Arsenic cannot be excreted from the human body, but instead accumulates in tissues with high keratin content such as skin, hair and nails [2,19].

Therefore, it is of great importance to detect arsenic, especially As (III), in water systems with high sensitivity and selectivity. As (III) is identified as one of the most harmful substances in water to human health, and it is 60 times more toxic than As (V) or organic arsenic compounds [20]. In order to protect our environment and ensure our health, it is imperative to develop a fast, low-cost and sensitive arsenic (III) detection method that is applicable to water environment.

Traditional methods for quantitative detection of heavy metal include atomic fluorescence spectrometry (AFS) [21], atomic absorption spectrometry (AAS) [22,23], inductively coupled plasma optical emission spectrometry (ICP-OES) [24,25], ICP-MS [26,27] and high performance liquid chromatography (HPLC) [28], etc. Although these methods can accurately measure arsenic in an environmental sample to microgram arsenic per liter concentrations, there is still a necessity for development of simple and rapid methods for field assays.

Sensors have great potential in high-throughput real-time detection of multiple heavy metal ions. Also, they needn't require tedious sample preparation, complex pretreatment procedures, expensive instruments and professional personnel. The rapid-developing nanotechnology has provided a new opportunity for improving the performance of sensors in terms of sensitivity, limit of detection, selectivity and reproducibility. Researchers first reported that Arsenic (III) can specifically bind to Arsenic (III) aptamer to form stable As (III)-aptamer complex in 2009 [3]. However, the following years saw few reports about biosensor of Arsenic (III) [29–31]. Zhou Pei et al. reported three methods for Arsenic (III) detection by combining Arsenic (III) aptamer with nanoparticles. Although they have successfully designed selective and sensitive aptamer biosensor for arsenic (III) detection in aqueous solution, it

* Corresponding author.
E-mail address: zhouxd@whu.edu.cn (X. Zhou).
[1] These authors contributed equally to the work.

http://dx.doi.org/10.1016/j.talanta.2015.08.052
0039-9140/

is still urgently needed to develop more sensitive, selective and environmentally friendly methods for Arsenic (III) detection in aqueous solution.

Surface-enhanced Raman scattering (SERS) technique, which can be used in conjunction with commercially available portable Raman systems, enjoys incomparable advantages and holds great potential in the future analysis and detection. Since its emergence in the 1980s [32–34], SERS has been widely applied to biomedical and environmental analysis at the level of molecules, pathogens, cells and even whole living animals [35–38]. The two well-known mechanisms of SERS are the electromagnetic (EM) enhancement mechanism and chemical enhancement or charge transfer (CT) enhancement mechanism [39,40]. SERS is an extremely sensitive analytical technique mainly based on the giant electromagnetic enhancement induced by localized plasmon resonance (LPR) of nanoscale noble metal surfaces [39]. Apart from its high sensitivity, SERS also possesses other inherent advantages, such as a wide range of excitation wavelengths, low photo-bleaching and high-resolution spectroscopic bands. Recently, the Au NPs-based SERS sensor has gained wide attention in the analysis and detection of DNA [41,42], heavy metal ions [43] and proteins [44]. Our research group also proposed a 'turn-off' SERS-based platform for ultrasensitive detection of thrombin with an unusual limit of detection (LOD) of 160 fM and a superwide detection range of 0.4–80 nM, which demonstrated the potential and superiority of this type of biosensor [45].

Based on all of these mentioned above, we proposed a novel SERS strategy for detection of As (III) with high selectivity and sensitivity. This SERS strategy combined As (III) aptamer with Raman labeled Au@Ag core–shell nanoparticles. In this work, Au@Ag had greatly enhanced the performance of SERS. 4-mercaptobenzoic acid (4-MBA) and As (III) aptamer were absorbed on Au@Ag to serve as a SERS donor. Scheme 1 shows the design of the assay for As (III). The As (III) added into homogeneous Raman labeled Au@Ag specifically bound to As (III) aptamer, making the aptamer displace from the surface of Au@Ag and subsequently leading to aggregation of Au@Ag. As a consequence, the signal of Raman reporter molecule 4-MBA was intensified due to the formation of SERS "hot spots". The addition of different concentrations of As (III) could result in corresponding amount of As (III) aptamer displaced from the surface of Au@Ag, and also corresponding aggregation degree of Au@Ag. Therefore, the signal intensity of 4-MBA can indicate different concentrations of As (III). It is based on this strategy that we successfully constructed a novel and simple As (III) biosensor with high selectivity and sensitivity.

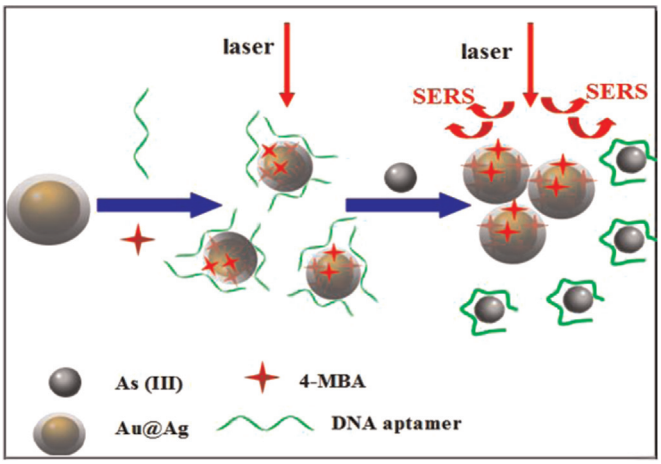

Scheme 1. Schematic representation of SERS detection of arsenic (III) based on Au@Ag core–shell nanoparticles.

2. Experiment

2.1. Reagents

(5'-GGTAATACGACTCACTATAGGGAGATACCAGCTTATTCAATTTT-ACAGAACAACCAACGTCGCTCCGGGTACTTCTTCATCGAGATAGTAAG-TGCAATCT-3') was purchased from Sangon Biotech (Shanghai, China) Co., Ltd. and purified by HPLC. N-(2-hydroxyethyl) piperazine-N-2-ethane sulfonic acid (HEPES) was bought from Jingke Hongda Biological Technology Co., Ltd. (Beijing, China). Trisodium citrate was obtained from Sigma-Aldrich (USA). $HAuCl_4 \cdot 3H_2O$ was purchased from Shanghai Chemical Reagent Co., Ltd. (Shanghai, China). 4-MBA was provided by Heowns Biochemical Technologies Co., Ltd. (Tianjin, China). As(III) and other substances to be detected (including Ni^{2+}, Cu^{2+}, Cr^{3+}, K^+, Na^+, Fe^{3+}, Pb^{2+}, Co^{2+}, Mn^{2+}, Hg^{2+}, Zn^{2+}, Al^{3+}, Fe^{2+}, Mg^{2+} and As (V) were prepared with ultrapure water from a Millipore system (resistivity of 18.2 MΩ cm). All glasswares were cleaned with aqua regia (volume ratio $HCl/HNO_3 = 3:1$) and rinsed with ultrapure water with an electrical resistivity greater than 18.2 MΩ cm throughout the experiment. All the experiments were carried out in 50 mM HEPES buffer solution of pH 7.2.

2.2. Apparatus

UV spectra of Au NPs and Au@Ag were obtained using a 500 μL quartz cell with a path length of 1 cm by UV-2550 spectrometer (Shimadzu, Japan). The morphology of Au@Ag was characterized by scanning electron microscope (SEM). Transmission Electron Microscope images of Au@Ag were obtained using a JEM-2100 (HR) microscope at an acceleration voltage of 200 kV. SERS spectra were obtained using a confocal microscope (Jobin Yvon HR-800, France) equipped with an air cooled charge-coupled device detector. He–Ne laser with 632.8 nm radiations was used for excitation. An Olympus 50 mm long working distance lens collected the scattering light to the charge-coupled device (CCD) detector. The slit width of the pinhole was set at 200 μm. The collecting parameters of each SERS spectrum were exposures time of 5 s and integrating twice over a spectral range from 600 to 1800 cm^{-1}. The pH measurements were carried out on a model UB-7 digital ion analyzer (Denver Instrument, America).

2.3. Synthesis of Au@Ag core–shell nanoparticles

Gold nanoparticles with a diameter of 30 nm were prepared by reduction of gold (III) chloride hydrate using trisodium citrate. To be specific, 50 mL 0.01% (w/w) $HAuCl_4$ was reduced by 750 μL 1% (w/w) trisodium citrate solution at 100 °C under vigorous magnetic stirring for 15–20 min until the solution turned from colorless to light red. The as-prepared red-colored Au particles were used as seed particles. Then 600 μL of $AgNO_3$ solution (0.5%, w/w) was added to 100 mL of boiling gold seed solution. Afterwards, 1 mL of sodium citrate solution (1%, w/w) was used as the reducing agent and added dropwise with stirring. The solution was boiled for 1 h and then heating was stopped. The Au@Ag core–shell nanoparticles were cooled down to room temperature.

2.4. Measurement procedures

The SERS measurements were carried out in the absence or presence of As (III) by using a Horbia Jobin Yvon Raman micro spectrometer. In a typical procedure, 100 nM As (III) aptamer solutions was added to Au@Ag solution to reach a final concentration of 5 nM. Then, 1 mM 4-MBA solution was added to the mixture to obtain a final concentration of 5 μM and react for some time. Afterwards, various concentrations of As (III) were mixed with the

modified Au@Ag solution (200 μL) at room temperature. A certain volume of HEPES buffer was added to the mixture to reach the final volume of 400 μL. The final concentration of As (III) was within the range of 0–100 ppb. The mixture reacted for 30 min allowing complete binding between As (III) aptamer and As (III). Finally, the reaction mixture was measured at room temperature.

3. Results and discussion

3.1. Characterization of AuNPs and Au@Ag

Au@Ag was synthesized by referring to the methods reported in previous literatures and making some modifications to them [46]. To confirm the successful synthesis of Au@Ag core–shell nanoparticles, the as-prepared Au@Ag was characterized by high resolution transmission electron microscopy (HRTEM) and SEM. As shown in Fig. 1A, the diameter of Au@Ag was approximately 40 nm exhibiting uniform size. Since AuNPs and Au@Ag of the same particle size had different UV absorption peaks, UV–vis spectrometer was used to further confirm that AuNPs were coated effectively by silver. Fig. 1B revealed the characteristics of AuNPs and Au@Ag. Compared with the absorption peak of AuNPs, the peak of Au@Ag solution was blue-shifted. According to these results, it was proved that we had successfully prepared Au@Ag in this work.

3.2. Detection mechanism

The detection mechanism for As (III) was illustrated in Scheme 1. As mentioned in some literatures, the colorimetric assay based on the surface plasmon resonance (SPR) of noble metal nanoparticles has drawn wide attention in recent years [47]. However, relatively less attention has been paid to SERS effect although many research groups have confirmed that the interstices of the aggregates of noble metal nanoparticles could more greatly enhance Raman intensity than that of the dispersed nanoparticles [48]. According to the assay for As (III) in Scheme 1, 4-MBA was modified onto Au@Ag via Au-S bonds. 4-MBA served as a Raman reporter molecule that provided simple and narrow characteristic peak. In this complex system, on the one hand, As (III) aptamer was effectively absorbed on Au@Ag by means of coordination interaction between N atom of base and Au@Ag. On the other hand, As (III) could specifically bind to As (III) aptamer to form As (III)-aptamer complex. In other words, As (III) competed with Raman labeled Au@Ag for binding to As (III) aptamer. As (III) added into homogeneous Raman labeled Au@Ag could specifically

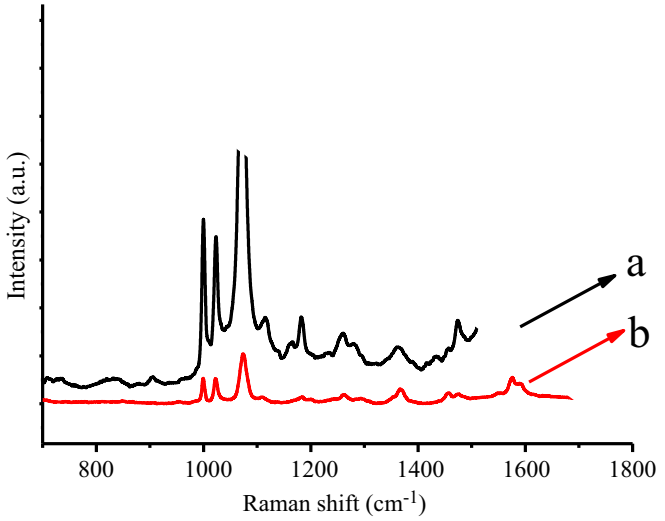

Fig. 2. The Raman spectra of 4-MBA (5 μM) in the absence of arsenic (III) (curve b) and the change of Raman spectra intensity in the presence of arsenic (III) (curve a) (10 ppb) due to aggregation of Au@Ag core–shell nanoparticles. All these Raman spectra were measured in HEPES buffer at room temperature.

bind to As (III) aptamer, making the aptamer displace from the surface of Au@Ag and ultimately leading to aggregation of Au@Ag. As a consequence, the signal intensity of Raman reporter molecule 4-MBA was significantly intensified due to the formation of SERS "hot spots" (As shown in Fig. 2).

3.3. Optimization of experimental parameters

In order to confirm the superior SERS effect of Au@Ag, we compared the different SERS signals of AuNPs and Au@Ag of the same particle diameter. Au@Ag nanoparticles were replaced by AuNPs of the same diameter. According to Fig. 3, the Raman intensity of 4-MBA absorbed on Au@Ag was much higher than that of 4-MBA absorbed on AuNPs. Previous literatures reported that Ag nanoparticles produce better SERS effect than gold nanoparticles. However, gold nanoparticles are not only well dispersed with uniform particle size, but also have low toxicity. Considering the advantages and disadvantages of such two kinds of nano materials, we successfully synthesized Au@Ag core–shell nanoparticles as SERS substrate and applied it to the As (III) detection system.

Considering the high dependence of SERS effect on the concentration of 4-MBA, we studied the effects of different

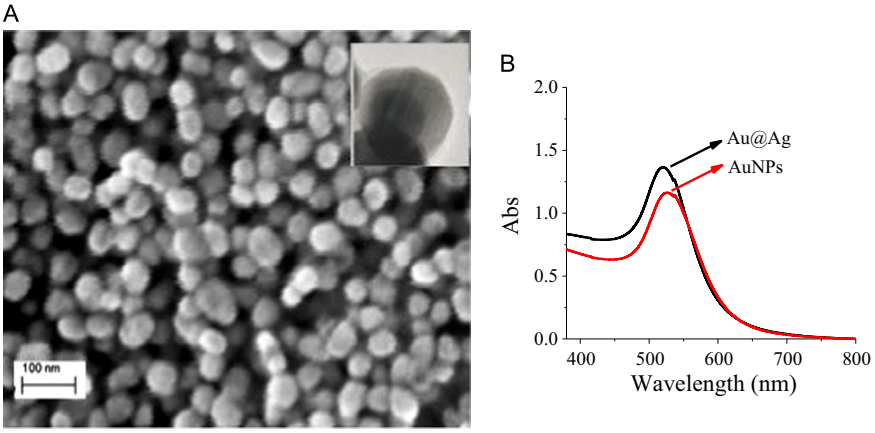

Fig. 1. Scanning electron microscope (SEM) image of as-prepared Au@Ag core–shell nanoparticles (the inset shows high resolution transmission emission microscope) (A) and UV–vis spectra of Au@Ag and AuNPs (B).

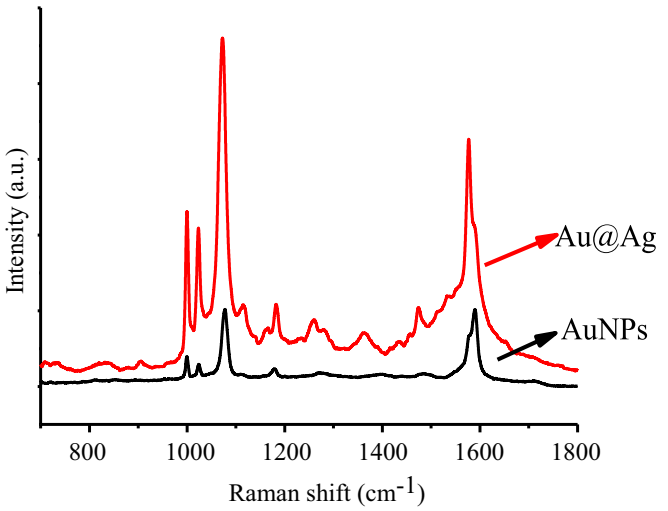

Fig. 3. The Raman spectra of 4-MBA absorbed on the surface of AuNPs and Au@Ag (100 nM As (III) aptamer solution was added to 200 μL AuNPs and Au@Ag solutions to reach a final concentration of 10 nM. Then, 1 mM 4-MBA solution was added to the mixture to obtain a final concentration of 5 μM, respectively. 10 ppb As (III) solution was mixed with the modified AuNPs and Au@Ag solution (200 μL) respectively. Finally, certain volumes of HEPES buffer were added to the mixture to reach the final volume of 400 μL, respectively.).

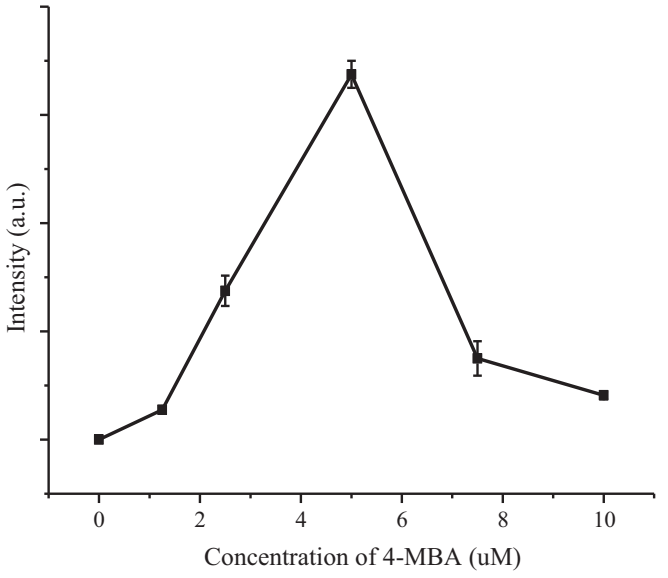

Fig. 4. Optimization of the concentrations of 4-MBA (100 nM As (III) aptamer solution was added to 200 μL Au@Ag solution to reach a final concentration of 10 nM. Then, different volumes of 1 mM 4-MBA solution were added to the mixture to obtain final concentrations of 0, 1.25, 2.5, 5, 7.5 and 10 μM, respectively. 5 ppb As (III) were mixed with the modified Au@Ag solution (200 μL). Finally, certain volumes of HEPES buffer were added to the mixture to reach the final volume of 400 μL.).

concentrations of MBA on Raman signal enhancement under certain concentration of As (III) aptamer. According to the Fig. 4, Raman intensity of MBA changed dramatically as the concentration of MBA increased from 0 to 10uM. According to previous reports, this is because too low concentration of MBA couldn't be absorbed on the surface of Au@Ag, resulting in low Raman intensity of MBA, while extremely high concentration of MBA may destroy the stability of the dispersed Au@Ag solution, contribute to serious aggregation of Au@Ag, and also cause low Raman intensity. Taking into account the effect of different concentrations of MBA on Raman intensity, 5 μM is the optimal concentration of 4-MBA.

3.4. SERS detection of As (III)

Different concentrations of As (III) was detected in the lab under the above optimized conditions. Under the optimized experimental conditions, the Raman spectra of the functionalized Au@Ag were obtained in the presence of 5 nM As (III) aptamer and different concentrations of As (III). The Raman reporter molecule employed in the experiment is 4-MBA, exhibited two obvious Raman bands at 1075 cm^{-1} and 1590 cm^{-1}. Moreover, the Raman intensity of these bands could be greatly enhanced when 4-MBA was located in "hot spots" region induced by aggregation of Au@Ag. In this experiment, 1075 cm^{-1} was chosen as the response signal of the SERS sensor to As (III). As shown in Fig. 5A, it was clearly indicated that the Raman intensity of SERS donor at 1075 cm^{-1} was gradually enhanced as the concentration of As (III) increased from 0 to 100 ppb in the presence of As (III) aptamer, owing to the increase of "hot spots" region. This result confirmed the coordination interaction between As (III) and As (III) aptamer. Fig. 5B showed the changes of Raman intensity of SERS donor at 1075 cm^{-1} with the concentration of As (III). It is found that the SERS intensity at 1075 cm^{-1} displays an excellent linear correlation with the concentration of As (III) ranging from 0.5 ppb to 10 ppb, as shown in the inset of Fig. 5B. The equation of linear regression was $y=619.80+489.67x$ (x is the concentration of As (III) and y is the Raman intensity at 1075 cm^{-1}), with a squared correlation coefficient of 0.992. The LOD of the SERS sensor for As (III) was calculated at 0.1 ppb according to the 3 times standard deviation rule. This indicates that the proposed assay for As (III) has satisfactory sensitivity due to the stronger Raman signals produced by the aggregation of functionalized Au@Ag.

3.5. Selectivity of the SERS sensor for As (III)

Other cations and anions, such as Ca^{2+} and Mg^{2+}, which can coexist with As (III) in natural waters may interfere with the detection of As (III). For this reason, we carried out selectivity test to explore the anti-interference performance of the proposed SERS sensor for As (III). The results were demonstrated in Fig. 6, showing that no other ions interfered with the detection of As (III) in natural waters. Furthermore, the effects of other 19 common ions were also taken into account. Typically, under the optimized experimental conditions, the As (III) detection system was added with 5 ppb As (III) and 500 ppb of other 19 other ions respectively. As shown in Fig. 6, the existence of other 19 common ions had almost no influence on detection of As (III). This suggested that the binding affinity of As (III) to As (III)-aptamer appears to be much stronger than that to all other ions except for As (V). The results demonstrated the high specificity of the proposed detection method for As (III).

3.6. Detection of As (III) in real sample

In order to further investigate the potential application of the newly-designed sensor in the practical samples, the assay was employed to detect As (III) in lake water. The water sample was chosen from the East Lake of Wuhan, Hubei Province, China. The water sample was first filtered by 0.22 μm microporous membrane. As shown in Table1, the concentration of As (III) in the lake water was 0.55 ppb. To verify the feasibility of this new As (III) detection method and get real concentration of As (III) in lake water, atomic absorption spectrometry (AAS) was applied to verify As (III) concentration in East Lake water compared with the As (III) probe in this work. Real concentration of As (III) detected by AAS in lake water is 0.594 ppb (SD=0.002, $n=3$). It can be seen from the result that we designed detection method corresponds well with the AAS result. According to Table 1, As (III) also had

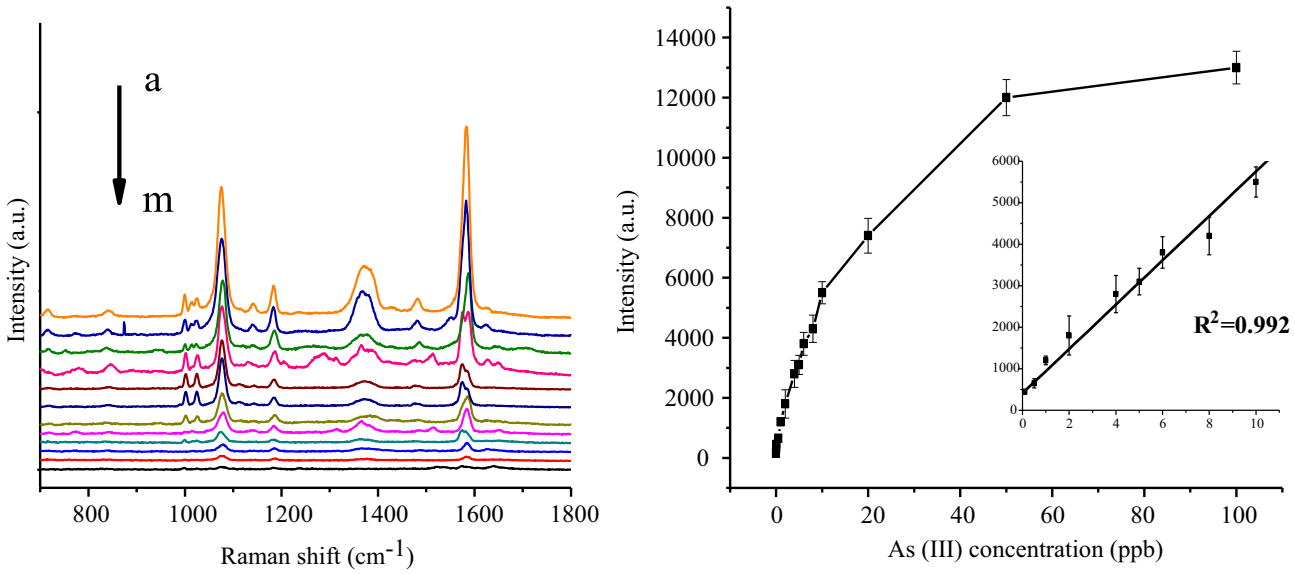

Fig. 5. (A) SERS spectra of SERS donor added with different concentrations of As (III) in the presence of 5 nM As (III)-aptamer, with concentrations of As (III) ranging from 10 to 0 ppb from top to bottom. (B) The Raman intensity of SERS donor at 1075 cm^{-1} varies with different concentrations of As (III) under optimized conditions. The inset shows the linear plot of the constant logarithm of Raman intensity at 1075 cm^{-1} under different concentrations of As (III) in HEPES buffer.

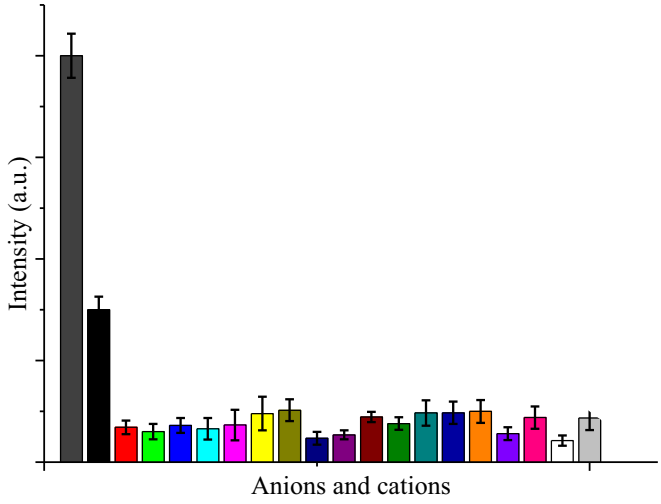

Fig. 6. Selectivity of the SERS sensor for As (III). The other 14 common metal ions and 5 common anions in natural waters instead of As (III) were used to react with above system and performed in the same way. The As (III) concentration of 5 ppb was tested, while the concentration of other inspected species was 500 ppb. All these experiments were operated at room temperature. Note: from left to right: As (III), As(V), SO_4^{2-}, NO_3^-, PO_4^{3-}, HCO_3^-, Ni^{2+}, Cu^{2+}, Cr^{3+}, K^+, Na^+, Fe^{3+}, Pb^{2+}, Co^{2+}, Hg^{2+},Zn^{2+}, Al^{3+}, Fe^{2+}, Mg^{2+} and Ag^+.

satisfactory rate of recovery at more than 84%. The detection limit of this assay for As (III) (0.1 ppb) was lower than the minimum limit guided by the United States Environmental Protection Agency (EPA) as well as that permitted by the World Health Organization (WHO). Therefore, this sensor demonstrated great potential in practical applications.

4. Conclusion

In summary, a simple and novel approach based on SERS and As (III) aptamer for detection of As (III) was proposed for the first time in this work. The proposed method has shown high sensitivity and selectivity for As (III) even in the presence of other competitive ions. More importantly, this highly sensitive and selective sensor may become an alternative method for As (III) detection in environment, biomedical field and other applications. Furthermore, we hope that this strategy based on Au@Ag as SERS substrate may offer a new approach for sensitive and selective detection of a wide spectrum of analytes and other metal ions or realize high-throughput drug screening only by changing corresponding aptamer.

Acknowledgment

We gratefully acknowledge the support from the Natural Science Foundation of China (NSFC) (No. 20927003, 90913013, 41273093 and 21175101), the National Major Scientific Instruments and Device Development Project (2012YQ16000701), and the Foundation of China Geological Survey (Grant no. 12120113015200).

Table 1
Rate of recovery of As (III). (100 nM As (III)-aptamer solution was added to 200 μL Au@Ag solutions to reach a final concentration of 5 nM. Then, 1 mM 4-MBA solution was added to the mixture to obtain a final concentration of 5 μM, respectively. As (III) solution was mixed with the modified Au@Ag solution (200 μL) and the final As (III) concentration were 2.00, 6.00 and 10.00 ppb respectively. Finally, certain volumes of lake water are added into the mixture, respectively.).

Added concentration of As (III) (ppb)	The measured concentration of As (III) (ppb)				Rate of standard recovery (%)			
–	$n=1$	$n=2$	$n=3$	Average	$n=1$	$n=2$	$n=3$	Average
0	0.52	0.48	0.64	0.55	–	–	–	–
2.00	2.34	2.26	2.23	2.28	89.50	85.50	84.00	86.33
6.00	6.25	6.31	5.84	6.13	95.00	96.00	88.17	93.06
10.00	10.36	10.44	10.01	10.27	98.10	98.90	94.60	97.20

Appendix A. Supplementary material

Supplementary data associated with this article can be found in the online version at http://dx.doi.org/10.1016/j.talanta.2015.08.052.

References

[1] S. Acharyya, P. Chakraborty, S. Lahiri, B. Raymahashay, S. Guha, A. Bhowmik, Nature 401 (1999) 545–547.
[2] I. Villaescusa, J.C. Bollinger, Rev. Environ. Sci. Biotechnol. 7 (2008) 307–323.
[3] M. Kim, H.J. Um, S. Bang, S.H. Lee, S.J. Oh, J.H. Han, K.W. Kim, J. Min, Y.H. Kim, Environ. Sci. Technol. 43 (2009) 9335–9340.
[4] D. Mohan, C.U. Pittman Jr, J. Hazard. Mater. 142 (2007) 1–53.
[5] M.M. Rahman, M.K. Sengupta, U.K. Chowdhury, D. Lodh, B. Das, S. Ahamed, D. Mandal, M.A. Hossain, S.C. Mukherjee, S. Pati, Arsenic contamination incidents round the world, in: R. Naidu, E. Smith, G. Owens, P. Bhattacharya, P. Nadebaum (Eds.), Managing Arsenic in the Environment: From Soil to Human Health, CSIRO publishing, Australia, 2006.
[6] M. Karim, Water Res. 34 (2000) 304–310.
[7] P. Mondal, C. Majumder, B. Mohanty, J. Hazard. Mater. 137 (2006) 464–479.
[8] P. Mondal, C. Balomajumder, B. Mohanty, J. Hazard. Mater. 144 (2007) 420–426.
[9] D. Chakraborti, M.M. Rahman, K. Paul, U.K. Chowdhury, M.K. Sengupta, D. Lodh, C.R. Chanda, K.C. Saha, S.C. Mukherjee, Talanta 58 (2002) 3–22.
[10] M.M. Hassan, Health Policy 74 (2005) 247–260.
[11] M. Hossain, Agric. Ecosyst. Environ. 113 (2006) 1–16.
[12] R. Nickson, J. McArthur, P. Ravenscroft, W. Burgess, K. Ahmed, Appl. Geochem. 15 (2000) 403–413.
[13] S. Zavareh, M. Zarei, F. Darvishi, H. Azizi, Chem. Eng. J. 273 (2015) 610–621.
[14] X. Xu, S. McGrath, A. Meharg, F. Zhao, Environ. Sci. Technol. 42 (2008) 5574–5579.
[15] A.H. Smith, C. Hopenhayn-Rich, M.N. Bates, H.M. Goeden, I. Hertz-Picciotto, H. M. Duggan, R. Wood, M.J. Kosnett, M.T. Smith, Environ. Health Perspect. 97 (1992) 259.
[16] R. Haque, D.G. Mazumder, S. Samanta, N. Ghosh, D. Kalman, M.M. Smith, S. Mitra, A. Santra, S. Lahiri, S. Das, Epidemiology 14 (2003) 174–182.
[17] R. Walvekar, S. Kane, M. Nadkarni, I. Bagwan, D. Chaukar, A. D'Cruz, J. Cutan. Pathol. 34 (2007) 203–206.
[18] C.H. Tseng, Atherosclerosis 199 (2008) 12–18.
[19] B.K. Mandal, Y. Ogra, K.T. Suzuki, Toxicol. Appl. Pharmacol. 189 (2003) 73–83.
[20] D.E. Mays, A. Hussam, Anal. Chim. Acta 646 (2009) 6–16.
[21] N. Zhang, N. Fu, Z. Fang, Y. Feng, L. Ke, Food Chem. 124 (2011) 1185–1188.
[22] N. Aksuner, V.N. TIRTOM, E. Henden, Turk. J. Chem. 35 (2011) 871–880.
[23] S. Sivrikaya, H. Altundag, M. Zengin, M. Imamoglu, Separ. Sci. Technol. 46 (2011) 2032–2040.
[24] V. Dufailly, L. Noël, T. Guérin, Anal. Chim. Acta 611 (2008) 134–142.
[25] E. Durduran, H. Altundag, M. Imamoglu, S.Z. Yıldız, M. Tuzen, J. Ind. Eng. Chem. 27 (2015) 245–250.
[26] H. Altundag, M.S. Dundar, Fresen. Environ. Bull. (2009) 98–101.
[27] H. Altundag, M.S. Dundar, Fresen. Environ. Bull. (2009) 2102–2107.
[28] K.H. Al-Assaf, J.F. Tyson, P.C. Uden, J. Anal. Atom Spectrom. 24 (2009) 376–384.
[29] Y. Wu, S. Zhan, F. Wang, L. He, W. Zhi, P. Zhou, Chem. Commun. 48 (2012) 4459–4461.
[30] Y. Wu, S. Zhan, H. Xing, L. He, L. Xu, P. Zhou, Nanoscale 4 (2012) 6841–6849.
[31] Y. Wu, L. Liu, S. Zhan, F. Wang, P. Zhou, Analyst 137 (2012) 4171–4178.
[32] M. Fleischmann, P. Hendra, A. McQuillan, Chem. Phys. Lett. 26 (1974) 163–166.
[33] D.L. Jeanmaire, R.P. Van Duyne, J. Electroanal. Chem. 84 (1977) 1–20.
[34] L. Chen, J. Choo, Electrophoresis 29 (2008) 1815–1828.
[35] E. KyuáLee, S. YoungáShin, S. WookáSon, C. HwanáOh, J. MyongáSong, S. HoáKang, Phys. Chem. Chem. Phys. 11 (2009) 7444–7449.
[36] X. Qian, X.-H. Peng, D.O. Ansari, Q. Yin-Goen, G.Z. Chen, D.M. Shin, L. Yang, A. N. Young, M.D. Wang, S. Nie, Nat. Biotechnol. 26 (2007) 83–90.
[37] S. Lee, J. Choi, L. Chen, B. Park, J.B. Kyong, G.H. Seong, J. Choo, Y. Lee, K.H. Shin, E.K. Lee, Anal. Chim. Acta 590 (2007) 139–144.
[38] R.M. Jarvis, R. Goodacre, Chem. Soc. Rev. 37 (2008) 931–936.
[39] M. Moskovits, Rev. Mod. Phys. 57 (1985) 783.
[40] A. Campion, P. Kambhampati, Chem. Soc. Rev. 27 (1998) 241–250.
[41] Z. Yi, X.Y. Li, F.J. Liu, P.Y. Jin, X. Chu, R.Q. Yu, Biosens. Bioelectron. 43 (2013) 308–314.
[42] Y.Z. Liu, Z.T. Wu, G.H. Zhou, Z.K. He, X.D. Zhou, A.G. Shen, J.M. Hu, Chem. Commun. 48 (2012) 3164–3166.
[43] Z. Krpetic, L. Guerrini, I.A. Larmour, J. Reglinski, K. Faulds, D. Graham, Small 8 (2012) 707–714.
[44] J. Neng, M.H. Harpster, W.C. Wilson, P.A. Johnson, Biosens. Bioelectron. 41 (2013) 316–321.
[45] Z. Wu, Y. Liu, X. Zhou, A. Shen, J. Hu, Biosens. Bioelectron. 44 (2013) 10–15.
[46] S. Ji, Z. Yang, C. Zhang, Z. Liu, W.W. Tjiu, I.Y. Phang, Z. Zhang, J. Pan, T. Liu, Electrochim. Acta 109 (2013) 269–275.
[47] S.K. Ghosh, T. Pal, Chem. Rev. 107 (2007) 4797–4862.
[48] K.L. Wustholz, A.-I. Henry, J.M. McMahon, R.G. Freeman, N. Valley, M.E. Piotti, M.J. Natan, G.C. Schatz, R.P.V. Duyne, J. Am. Chem. Soc. 132 (2010) 10903–10910.